INFECTION AND IMMUNITY, Jan. 2006, p. 673–681 Vol. 74, No. 1
0019-9567/06/$08.00+0 doi:10.1128/IAI.74.1.673–681.2006

$CD4^+$-T-Cell Effector Functions and Costimulatory Requirements Essential for Surviving Mucosal Infection with *Citrobacter rodentium*

Lynn Bry,[1,2]* Manfred Brigl,[1] and Michael B. Brenner[1]

Lymphocyte Biology Section, Division of Rheumatology, Immunology and Allergy, Department of Medicine,[1] and Department of Pathology, Brigham & Women's Hospital,[2] Harvard Medical School, Boston, Massachusetts 02115

Received 14 June 2005/Returned for modification 21 September 2005/Accepted 24 October 2005

Citrobacter rodentium **causes an attaching and effacing infection of the mouse colon. Surprisingly, protective adaptive immunity against this mucosal pathogen requires a systemic T-cell-dependent antibody response. To define $CD4^+$ T-cell effector functions promoting this systemic defense of infected epithelial surfaces, studies were undertaken in weaning-age mice lacking costimulatory molecules CD28 or CD40L or cytokines gamma interferon (IFN-γ) or interleukin-4 (IL-4). Adoptive transfer of $CD4^+$ T cells from wild-type, $CD28^{-/-}$, $CD40L^{-/-}$, or IFN-$\gamma^{-/-}$ donors to $CD4^{-/-}$ recipients delineated functions of these $CD4^+$ T-cell-expressed molecules on the outcome of infection. Wild-type and IL-$4^{-/-}$ mice successfully resolved infection, while 70% of IFN-$\gamma^{-/-}$ mice survived. In contrast, all $CD28^{-/-}$ mice succumbed during acute infection. While fewer than half of $CD40L^{-/-}$ mice succumbed acutely, surviving mice failed to clear infection, resulting in progressive mucosal destruction, polymicrobial sepsis, and death 1 to 2 weeks later than in $CD28^{-/-}$ mice. Downstream of CD28-mediated effects, $CD4^+$ T-cell-expressed CD40L proved essential for generating acute pathogen-specific immunoglobulin M (IgM) and early IgG, which reduced pathogen burdens. However, deficiency of $CD4^+$ T-cell-expressed IFN-γ did not adversely impact survival or development of protective antibody in adoptively transferred $CD4^{-/-}$ recipients, though it impacted Th1 antibody responses. These findings demonstrate that $CD4^+$ T-cell-expressed CD40L promotes the rapid production of protective systemic antibody during acute infection, while deficiencies of IL-4 or of $CD4^+$ T-cell-expressed IFN-γ can be overcome. These findings have important implications for understanding the role of T-helper-cell responses during infections involving mucosal surfaces.**

Citrobacter rodentium serves as the mouse model for studying the pathogenesis and host responses to attaching and effacing pathogens. These pathogens cause significant morbidity and mortality among infants and children in the developing world and among animals of agricultural significance. As with related pathogens, including the enteropathogenic *Escherichia coli*, *C. rodentium* causes a self-limited infection of the apical surface of the gut epithelium (2, 14, 16). The noninvasive nature of this infection provides a model for dissecting events associated with infections of mucosal surfaces, including the host responses needed to resolve them. This infection also serves as the primary mouse model of infectious colitis, providing a rigorous system for understanding microbial contributions to gut inflammation and pathways involved in its successful resolution.

Primary infection with *C. rodentium* progresses through three distinct phases, a useful schema for defining points at which elements of innate and adaptive immunity impact host defense. First, colonization and proliferation of the pathogen start with successful introduction of *C. rodentium* into the colon. After initial adhesion (4), attaching and effacing lesions form, mediated by the bacterial adhesin intimin and type III secreted bacterial proteins, including the translocated intimin receptor, Tir (7, 8, 18). Innate defenses, including epithelial-produced β-defensins, affect early colonization and proliferation of *C. rodentium* in the colon (13, 24). The presence of mucosal antibody also appears to impact the initial kinetics of bacterial growth (2, 15, 28). Second, by the onset of symptomatic infection 7 to 10 days after inoculation, the developing pathogen burden has triggered a number of epithelial responses, including the hallmark hyperplastic response and production of antimicrobial factors (14, 24). Previous studies have also demonstrated protective roles for proinflammatory cascades resulting in secretion of gamma interferon (IFN-γ) and tumor necrosis factor alpha member cytokines in the colon (9, 10, 24, 26). Interestingly, acute infection primarily recruits $CD4^+$ T cells into the colon, though abscess formation in proximity to densely colonized areas intermittently disrupts epithelial integrity, creating the potential for polymicrobial sepsis as *C. rodentium* and lesser numbers of commensals gain entrance to host tissues (2). While adult immunocompetent hosts control this aspect of the infection, it contributes to the lethality and morbidity seen in immature animals and populations with defects in B cells and $CD4^+$ T cells (2, 25). Third, most mice resolve infection within 4 weeks after initial inoculation. Immunocompetent hosts clear the pathogen, with resolution of inflammation and return of epithelial proliferation to a baseline state.

The development of T-cell-dependent serum antibody

* Corresponding author. Mailing address: 4226-EBRC, Department of Pathology, Brigham & Women's Hospital, Harvard Medical School, Boston, MA 02115. Phone: (617) 732-7763. Fax: (617) 264-6898. E-mail: lbry@partners.org.

proved the critical adaptive response needed to survive and resolve this primary infection of a mucosal surface (2). This response consists of $CD4^+$ T-cell-dependent serum immunoglobulin M (IgM) and evolving IgG predominated by the Th1-biased isotype IgG2c, the IgG2a allotype produced in C57BL/6 mice. Surprisingly, this response did not require $CD4^+$ T-cell or B-cell responses in mucosal tissues, as evidenced by survival and resolution of infection in mice lacking β_7-integrins, adhesion molecules facilitating binding of lymphocytes to the mucosal addressing cell adhesion molecule (MAdCAM) that permits entry into mucosal sites, including the GALT (2). These findings indicate that protective adaptive responses against attaching and effacing pathogens do not need to occur in the same tissue compartment as the primary site of infection.

Activation of naïve T cells through costimulatory molecules such as CD28 or ICOS leads to the expression of downstream effector costimulatory molecules, including CD40L, OX40, and CD27, each of which impacts Th1/Th2 differentiation, cytokine production, and end effects on B-cell stimulation, germinal center formation, and antibody production (1, 11, 12, 21, 29, 30).

However, when framed in the context of infection with a noninvasive mucosal pathogen, we know remarkably little regarding how these $CD4^+$ T-cell effector functions facilitate host survival and resolution of infection. We thus undertook infection studies with mice lacking CD28, CD40L, IFN-γ, or interleukin-4 (IL-4), molecules with potential impact on host defense against *C. rodentium*. Adoptive transfer of wild-type $CD28^-$, $CD40L^-$, or IFN-γ^- $CD4^+$ T cells into $CD4^{-/-}$ recipients subsequently elucidated the functional roles of these $CD4^+$ T-cell-expressed molecules on the generation of protective antibody, control of pathogen burdens, and resolution of infection. We found that CD28 and CD40L were dominant in providing T-cell help for protective antibody responses, while single deficiency of IL-4 or of $CD4^+$ T-cell-expressed IFN-γ did not produce an appreciable impact upon successful resolution of infection.

MATERIALS AND METHODS

Bacterial strains. *Citrobacter rodentium* strain DBS 100 and mouse commensal *E. coli* cells were cultured on MacConkey agar (Remel Inc.) or in Luria-Bertani (LB) broth (2).

Mouse strains. $CD45.1^+$ and $CD45.2^+$ wild-type and $CD45.2^+$ $CD28^{-/-}$, $CD40L^{-/-}$, IFN-$\gamma^{-/-}$ IL-$4^{-/-}$, and $CD4^{-/-}$ C57BL/6 mice were obtained from Jackson Laboratories (Bar Harbor, ME), housed as previously described (2). All methods and procedures were carried out in accordance with Animal Care and Use Committee-approved protocols.

Infection of mice. Weaning-age mice were fasted 8 h prior to oral inoculation with 5×10^8 CFU of *C. rodentium*. Animals were allowed access to food after inoculation. All manipulations were performed in BL-2 biosafety cabinets. During infection, moribund animals or those showing unalleviated distress were euthanized.

Survival studies. A least six mice of each C57BL/6 strain were analyzed in a minimum of two independent experiments. Log rank and chi-square analyses were carried out in Prism 4.0 to determine median survival time and statistical significance. A P value of <0.05 was considered significant.

Tissue collection, histology, and immunofluorescence. Samples of spleen, liver, mesenteric lymph node (MLN), small intestine, and colon were placed in 10% Formalin in phosphate-buffered saline (PBS), or in tissue blocks containing OCT (Tissue-Tek) and snap-frozen. The colon was dissected to the anal canal and removed en bloc. Five-micrometer sections were stained with hematoxylin and eosin. Immunofluorescent staining was performed on frozen sections fixed in cold methanol for 5 min, washed in PBS, and blocked for 10 min in PBS plus 5% mouse serum prior to staining with rat anti-mouse E-cadherin (Zymed) and recognized with rabbit anti-rat Ig conjugated to AMCA (Jackson Immunochemical), hamster anti-mouse CD3ε conjugated to fluorescein isothiocyanate (FITC) (Caltag), rat anti-mouse CD4 conjugated to phycoerythrin (PE; Caltag), rat anti-mouse CD45.1-FITC (eBiosciences), and Hoechst nuclear dye (bis-benzimide; Sigma Chemical; 1 mg/ml stock solution diluted 1:10,000).

Colony counts. Distal colon, spleen, and liver were weighed, homogenized, serially diluted, and plated in triplicate to MacConkey agar. *C. rodentium* and *E. coli* colonies were counted after 24 h of incubation at 37°C to determine $\log_{10}$ CFU per gram of tissue. Lower detection limits were 20 CFU/gram spleen ($\log_{10} = 1.3$), 8 CFU/gram liver ($\log_{10} = 0.9$), and 12 CFU/gram colon or fecal pellets ($\log_{10} = 1.1$).

Preparation of serum and fecal lysates. Serum prepared from whole blood was collected by periorbital eye bleed from sevoflurane-anesthetized mice. For preparation of fecal lysates, fecal pellets were collected from mice, weighed, and subjected to two sequential extractions in fecal lysate extraction buffer (0.1% Tween 20 plus 10 μl Sigma protease inhibitors/ml); 0.5 ml of buffer was added per 0.1 g of material for each extraction. Material was vortexed for 20 min and spun for 10 min at 12,000 rpm, and supernatant was passed over a 0.22-μm-filter spin tube (Corning). Sequentially collected supernatants from the same sample were pooled to result in 1 ml of lysate per 0.1 g of fecal material.

Immunoglobulin enzyme-linked immunosorbent assays. Antibody enzyme-linked immunosorbent assays were performed by coating 96-well plates with heat killed *C. rodentium*. Plates were incubated overnight washed with PBS plus 0.05% Tween 20, blocked in 10% soy milk (8th Continent) plus PBS plus 0.05% Tween 20 and washed prior to addition of serially diluted serum or fecal lysates. Samples were incubated for 2 h at room temperature and washed, and bound antibody was detected with goat anti-mouse IgA, IgM, IgG1, IgG2b, IgG2c, or IgG3 (Southern Biotechnology Associates) conjugated to alkaline phosphatase. After 1 h of incubation at room temperature, washed plates were developed with *p*-nitrophenyl phosphate (PNPP; Sigma), read in a Molecular Devices reader, and analyzed in SoftMAX 4.0 with a four-parameter fit of mean absorbance at an optical density of 405 nm of each sample versus the reciprocal of the dilution. Interpolation with the resulting equation was used to define the relative endpoint titer yielding an optical density of 405 nm of 0.15. The minimum detectable titer was 50.

Serum transfers. Adoptive transfer of serum from mice was performed as previously described (2). Briefly, wild-type, $CD40L^{-/-}$, or IFN-$\gamma^{-/-}$ donors were infected 2 weeks prior to $CD4^{-/-}$ recipients. On days 3, 4, and 5 after inoculation of $CD4^{-/-}$ recipients with *C. rodentium*, whole blood was collected from acutely infected donors, allowed to clot, and filter sterilized prior to immediate administration of 0.25 ml serum to each recipient. Each $CD4^{-/-}$ recipient received serum only from wild-type, $CD40L^{-/-}$, or IFN-$\gamma^{-/-}$ donors to assess the protective capacity of the acute antibody responses in donor mice. Survival of $CD4^{-/-}$ recipients was monitored for 6 weeks after infection with *C. rodentium*.

T-cell purification. Spleen and mesenteric lymph node were harvested from naïve 5-week-old $CD45.1^+$ or $CD45.2^+$ wild-type mice or $CD45.2^+$ $CD28^{-/-}$, $CD40L^{-/-}$, or IFN-$\gamma^{-/-}$ C57BL/6 mice. Tissues were macerated through a 70-μm mesh filter (Becton Dickinson) into 10 ml of RPMI plus 10% calf serum (R10; Gibco). Cells were spun for 5 min at 1,500 rpm at 4°C, and red cells were lysed. Preparations were spun and washed with R10, and the cell concentration was determined. Control preparations were suspended to deliver 20 million unfractionated cells to recipient mice. Remaining cells were suspended to 2.5×10^8 cells/ml for purification with $CD4^+$ or $CD8^+$ T-cell magnetic bead purification kits, performed per the manufacturer's specifications (Miltenyi). Purified cells were stained with rat anti-mouse CD4, CD8α, CD19, GR1, F4/80, or rat isotype control conjugated to phycoerythrin (Caltag) and analyzed on a Becton-Dickinson fluorescence-activated cell sorter (FACS) Scan device. $CD4^+$ T-cell preparations gave ≥96% $CD4^+$ T cells, ≤1% $CD19^+$ B cells, <1% $CD8^+$ T cells, <1% $F4/80^+$ macrophages, or $GR1^+$ neutrophils and ≤1% dead cells. The resulting suspensions were passed over a 40-μm mesh filter and suspended in RPMI to deliver ~5 million cells per recipient mouse at 23 days of age. Recipients were orally inoculated with *C. rodentium* as described 2 days after adoptive transfer. Administration of 5 million purified $CD4^+$ T cells conferred a significant survival phenotype in $CD4^{-/-}$ recipients infected with *C. rodentium*, but administration of 20 million unfractionated cells, 5 million $CD8^+$ T cells, or 500,000 $CD4^+$ T cells did not.

FACS analysis of tissues from adoptively transferred mice. Tissues from wild-type, control, and adoptively transferred $CD4^{-/-}$ recipients were obtained at day 15 postinoculation (day 17 posttransfer). Spleen and MLN were macerated through 70-μm filters. Distal colon was opened and flushed with cold Hanks buffered saline solution (Gibco) and placed on parafilm, and the mucosa was gently scraped with a sterile razor blade. Scraped material was placed in cold HBSS, pelleted at 1,500 rpm prior to two 15-min incubations at 37°C in HBSS

plus 10% fetal calf serum (FCS) plus antibiotics plus 2 mM EDTA to release epithelial cells from stromal cells. Material was resuspended in R10 plus type IV collagenase (dispase) plus 10 U/ml of DNase (Pierce) and underwent two 20-min incubations at 37°C. Collected fractions were passed over 40-μm Nytex mesh filters, spun, washed twice in R10, and resuspended for staining with species and isotype-specific controls (Caltag), hamster anti-mouse CD3e-cychrome (Pharmingen), CD4-PE or -FITC, CD8α-PE or -FITC, CD19-PE, F4/80-PE, and FITC-conjugated anti-mouse CD45.1 or CD45.2 (eBiosciences). In mice receiving purified $CD45.1^+$ $CD4^+$ T cells, $CD8^+$, $CD19^+$, or other $CD45.1^+$ cells remained at <0.5% at 15 days after transfer. By FACS analysis, cells within the lymphocyte gate were gated by CD3 positivity in FL-3 and analyzed for CD4 or CD8α expression in FL-1 to determine the percentages of $CD4^+$ and $CD8^+$ T cells from these locations. Mice adoptively transferred with $CD45.1^+$ cells were gated on $CD45.1^+$ in the FL-1 channel and analyzed in FL-2 for CD4 expression and FL-3 for CD3 expression to determine the phenotype of the transferred cell populations.

RESULTS

IFN-γ, CD28, and CD40L impact survival of infection with *C. rodentium*. Survival studies with wild-type, $CD28^{-/-}$, $CD40L^{-/-}$, IFN-$\gamma^{-/-}$, and IL-$4^{-/-}$ mice defined critical junctures during infection requiring expression of these molecules. Animals were infected at 21 days of age, a time during which mice are more susceptible to infection with *C. rodentium* and one modeling the development of symptomatic infections caused by attaching-and-effacing pathogens in susceptible populations, including human children and young animals. Whereas all wild-type (Fig. 1A) and IL-4-deficient (Fig. 1B) mice survived infection, 100% of $CD28^{-/-}$ mice succumbed during acute infection (Fig. 1C). While 40% of $CD40L^{-/-}$ animals succumbed during acute infection (Fig. 1D), the remaining 60% succumbed over the next 2 weeks, during the time that wild-type mice cleared *C. rodentium* from the colon. IFN-$\gamma^{-/-}$ mice demonstrated 30% lethality during acute infection with survival of remaining animals (Fig. 1E). These findings indicated that costimulatory events mediated by CD28 impacted necessary host responses during acute infection. Surprisingly, costimulation mediated by CD40L impacted events associated with both acute and resolution stages of infection, while deficiency of IFN-γ demonstrated a milder but still important contribution toward survival of acute infection.

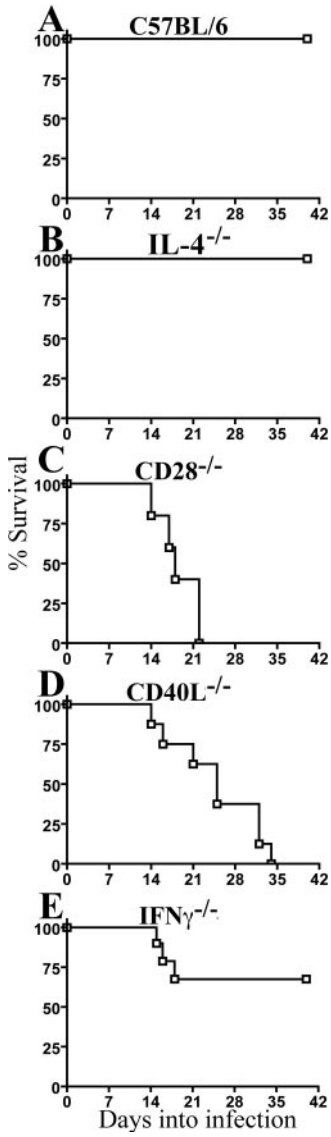

FIG. 1. Survival among mice lacking CD28, CD40L, IL-4, or IFN-γ. Mice were orally inoculated with 5×10^8 CFU of *C. rodentium* at day 21 of age. (A) Wild-type C57BL/6 mice (n = 12 mice). (B) IL-$4^{-/-}$ mice (n = 6 mice). (C) $CD28^{-/-}$ mice (n = 6 mice). (D) $CD40L^{-/-}$ mice (n = 9 mice). (E) IFN-$\gamma^{-/-}$ mice (n = 7 mice).

Deficiency of CD28 or CD40L leads to development of polymicrobial sepsis, damage to colon and internal organs, and defects in bacterial clearance. Wild-type mice characteristically develop peak pathogen burdens 2 weeks into infection, with numbers exceeding 1×10^8 CFU of *C. rodentium* per gram of colon (Fig. 2A). In spite of this pathogen burden, the colonic epithelium remains grossly intact with rare breaks associated with abscess formation and efflux of neutrophils into the lumen (Fig. 3A) (2). The pathogen burden declines 3 to 4 logs over the next week, with the majority of animals clearing *C. rodentium* within 4 weeks (Fig. 2A and 3E). The same pattern was found in mice lacking IL-4 (data not shown).

All knockout strains demonstrated colonic burdens of *C. rodentium* similar to those of wild-type mice during initial colonization and proliferation (Fig. 2A to D). By 15 days of infection, $CD28^{-/-}$ mice demonstrated a half-log-higher colonic burden of *C. rodentium* than wild-type or other knockout strains of mice (Fig. 2B). Histologically, the distal colon of $CD28^{-/-}$ mice also demonstrated more frequent focal abscesses and breaks in epithelial integrity than those found in wild-type or IFN-γ- or CD40L-deficient mice (Fig. 3A to D) (data not shown). However, while pathogen burdens in wild-type mice dropped >3 logs between 15 and 21 days of infection (Fig. 2A), the pathogen burden remained constant or rose in surviving $CD40L^{-/-}$ mice (Fig. 2C). This failure to clear the colonic infection was associated with increasing destruction of the gut mucosa (Fig. 3F). The pathogen burden in IFN-$\gamma^{-/-}$ mice remained comparable to that in wild-type mice, except for a mean 10-day lag in clearance of colonic *C. rodentium* and delayed resolution of mucosal inflammation (Fig. 2D and 3G and H).

Investigation of CFU in liver and spleen revealed key defects. Prior studies in mice lacking $CD4^+$ T cells demonstrated worsening polymicrobial sepsis by day 15 of infection, characterized by systemic spread of *C. rodentium* and lesser numbers

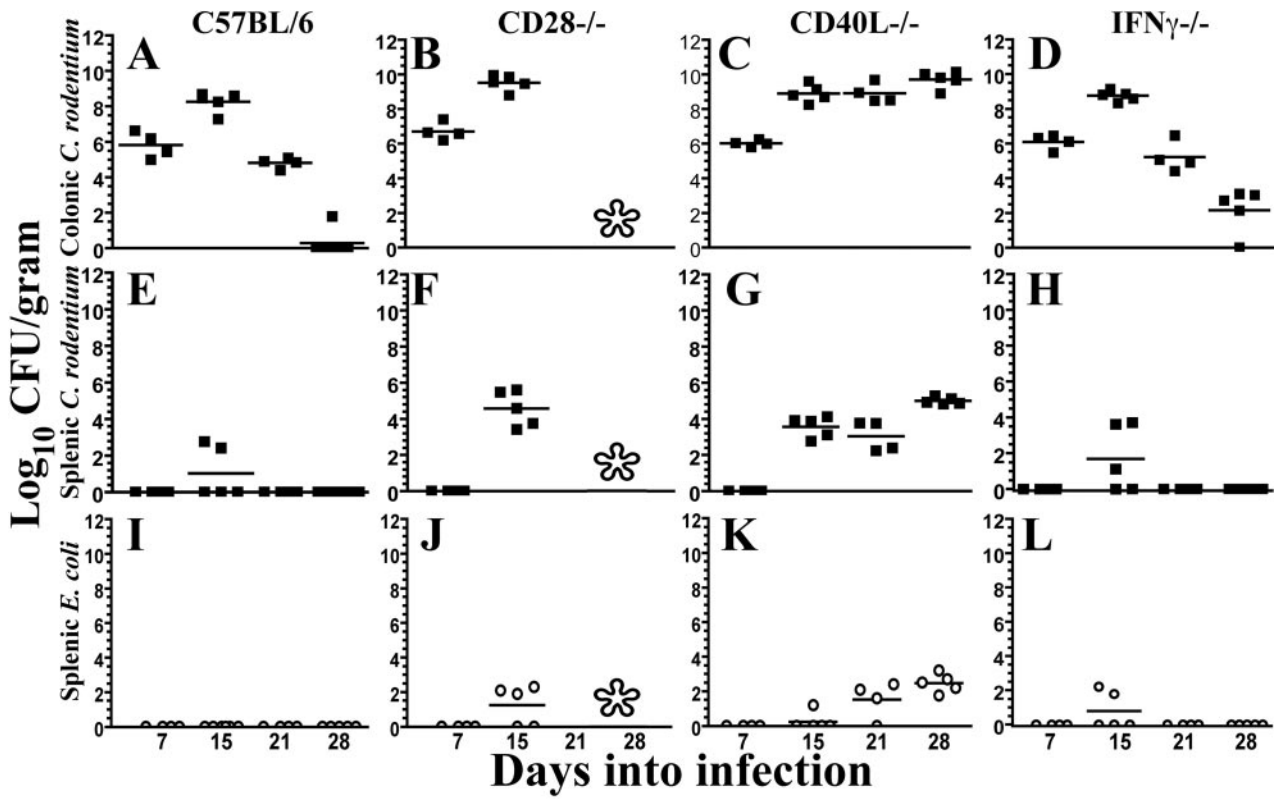

FIG. 2. Pathogen burden in colon and spleen. The *x* axis denotes the number of days into infection. The *y* axis denotes $\log_{10}$ CFU of *C. rodentium*/gram of colon (A to D) or spleen (E to H) or *E. coli* in spleen (I to L). Lower limits of detection are 20 CFU/gram spleen and 12 CFU/gram colon. An asterisk indicates no surviving mice at those time points for analysis. Squares, CFU of *C. rodentium*; open circles, CFU of *E. coli*.

of commensal species (2), events that were infrequent in wild-type mice (Fig. 2E and I). CD28$^{-/-}$ mice demonstrated a similar septic picture characterized by the presence of *C. rodentium* and commensal *E. coli* in spleen and liver (Fig. 2F and J). The liver in particular demonstrated frequent focal abscesses and hepatocyte damage (Fig. 3J). CD40L$^{-/-}$ mice developed a milder septic picture (Fig. 2G and K) with less damage to internal organs by day 15 of infection (Fig. 3K). However, at later time points, numbers of *C. rodentium* and *E. coli* increased in CD40L$^{-/-}$ mice (Fig. 2G and K) as did damage to internal organs, liver in particular (Fig. 3L). In contrast, IFN-$\gamma^{-/-}$ mice displayed milder sepsis acutely that resolved in surviving animals (Fig. 2H and L).

T-cell costimulation mediated by CD28 and CD40L is required for development of protective antibody responses against *C. rodentium*. We next determined the effect of CD28, CD40L, or IFN-γ deficiency on acute antibody responses against *C. rodentium*. Wild-type mice infected with *C. rodentium* characteristically develop strong pathogen-specific serum IgM responses that peak approximately 2 weeks after oral inoculation (Fig. 4A, squares). IgG responses rise above baseline and peak over subsequent weeks (2). The IgG responses at day 15 of infection in wild-type mice demonstrate rising production of IgG2b (Fig. 4C) and Th1-dependent IgG2c (Fig. 4D).

In contrast to the early antibody profile seen in wild-type mice, CD28-deficient mice failed to mount significant pathogen-specific antibody at 15 days of infection (Fig. 4A to E, triangles). Lack of CD40L impaired the production of acute-pathogen-specific IgM (Fig. 4A, triangles) and IgG, with the exception of minimal titers of IgG2b at day 15 (Fig. 4D). This lack of significant IgG reactivity persisted in CD40L$^{-/-}$ mice surviving beyond day 15 of infection (data not shown). IFN-$\gamma^{-/-}$ mice developed total pathogen-specific Ig responses comparable to those of wild-type mice, with IgG2b (Fig. 4D, diamonds) and/or IgG3 (Fig. 4E) developing in the absence of IgG2c (Fig. 4C).

Analyses of immunoglobulin titers in feces demonstrated a similar striking impact on the development of *C. rodentium*-specific antibody that reached the bowel lumen. At day 15 of infection, wild-type and IFN-$\gamma^{-/-}$ mice demonstrated comparable titers of reactive fecal IgM, IgA, and IgG2b, the primary IgG isotype detected. In contrast, CD28$^{-/-}$ mice demonstrated limited fecal IgA responses, in the absence of detectable anti-*Citrobacter* IgG (Fig. 4F to J). Likewise, titers of reactive fecal IgM, IgA, and IgG were significantly reduced in CD40L$^{-/-}$ mice. Though CD40L$^{-/-}$ mice produced detectable IgG2b against *C. rodentium* (Fig. 4H), these titers were 10-fold lower than those found in wild-type or IFN-$\gamma^{-/-}$ mice.

We next assessed the protective capacity of the acute-phase serum Ig responses produced in CD40L- and IFN-γ-deficient mice. Previous studies demonstrated that administration of serum or purified serum Ig from infected wild-type donors to highly susceptible CD4$^{-/-}$ mice protected recipients from infection with *C. rodentium* (2). As shown in Fig. 5A, transfer of wild-type acute-phase serum protected 100% of CD4$^{-/-}$ re-

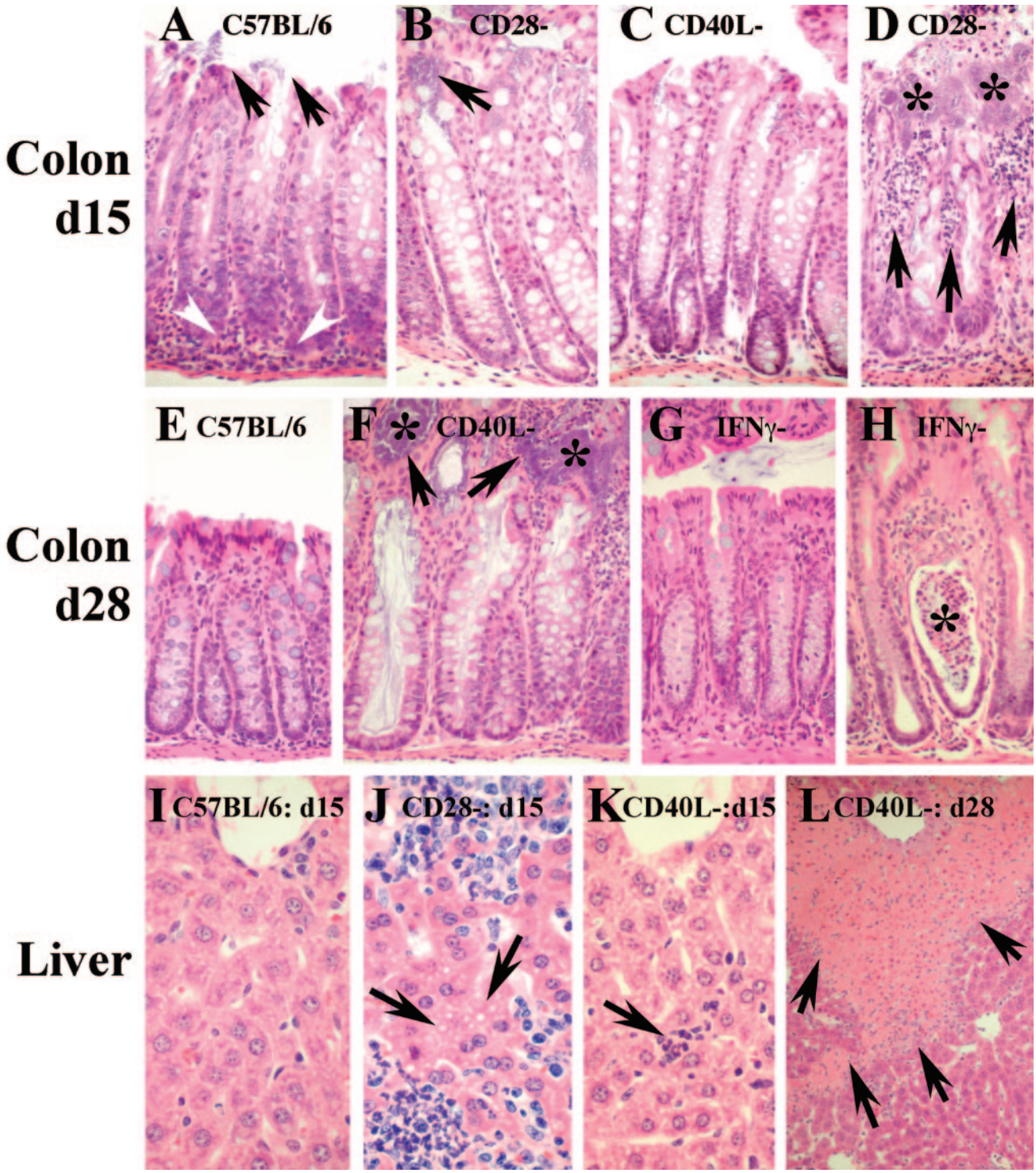

FIG. 3. Tissue pathology in infected mouse strains. Shown are hematoxylin and eosin stains at a ×200 magnification unless otherwise noted. (A) Colon of C57BL/6 mouse at day 15 of infection showing adherent *C. rodentium* (arrows) and lymphocytic infiltrate near the epithelial crypts (arrowheads). The epithelium remains intact. (B) Adherent *C. rodentium* (arrow) in a CD28$^{-/-}$ mouse. (C) CD40L$^{-/-}$ mouse at day 15. (D) Area of disrupted epithelium in a CD28$^{-/-}$ mouse at 15 days into infection. Asterisks indicate microcolonies of *C. rodentium* in the lamina propria. Arrows point to abscesses and epithelial disruptions. (E) Colon of wild-type mouse 28 days into infection. *C. rodentium* cells have been cleared, and epithelial hyperplasia has largely resolved, though remnants of the crypt-associated inflammatory infiltrate remain. (F) Colon of CD40L$^{-/-}$ mouse at 28 days showing mucin-engorged crypts, epithelial disruptions (arrows), and microcolonies of *C. rodentium* contacting the mucosa (asterisk). (G) Colon from IFN-γ$^{-/-}$ mouse (similar to panel E). (H) Rare lamina propria microabscess in IFN-γ$^{-/-}$ mouse 28 days into infection with sloughed cells in the crypt lumen (asterisk). (I to L) Liver at ×400. (I) Clear hepatic sinusoid from wild-type mouse at day 15 of infection. The top of the image shows the central vein. (J) Sinusoids from CD28$^{-/-}$ mouse demonstrating abscess formation. Arrows point to an area of ballooning degeneration. (K) Section from CD40L$^{-/-}$ mouse similar to panel I, but demonstrating a small microabscess (arrow). (L) A ×100 image of liver from a CD40L$^{-/-}$ mouse at day 28 showing widespread geographic necrosis (arrows) extending from regions supplied by the portal circulation.

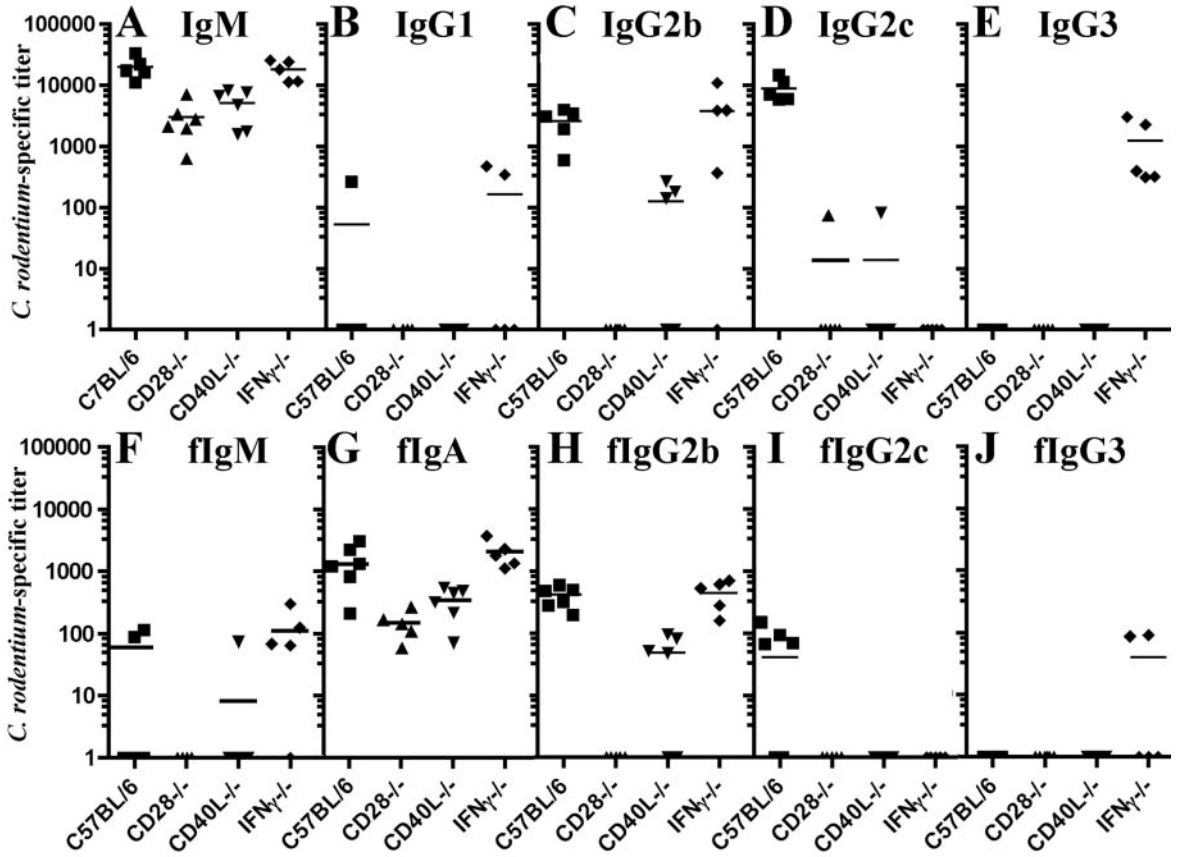

FIG. 4. Anti-*C. rodentium* serum and mucosal Ig responses: the *x* axis denotes mouse strains, and the *y* axis shows relative endpoint titers. Bars indicate mean values. Squares, wild-type C57BL/6 mice; triangles, CD28$^{-/-}$ mice; inverted triangles, CD40L$^{-/-}$ mice; diamonds, IFN-$\gamma^{-/-}$ mice. (A to E) Serum antibody responses against *C. rodentium* at day 15 of infection. (A) IgM. (B) IgG1. (C) IgG2b. (D) IgG2c. (E) IgG3. (F to J) Mucosal antibody responses against *C. rodentium* at day 15. (F) Fecal IgM. (G) IgA. (H) IgG2b. (I) IgG2c. (J) IgG3. The minimum detectable titer is 50.

cipients, as did transfer of serum from IFN-$\gamma^{-/-}$ donors. While serum transfer from CD40L$^{-/-}$ mice provided a survival advantage of 7.45 days, it failed to protect CD4$^{-/-}$ recipients. These data indicate that the limited pathogen-specific Ig response produced in CD40L$^{-/-}$ mice extends survival of CD4$^{-/-}$ recipients but fails to provide complete protection. Though IFN-γ impacts the profile of reactive IgG, its production was not required to generate protective antibody.

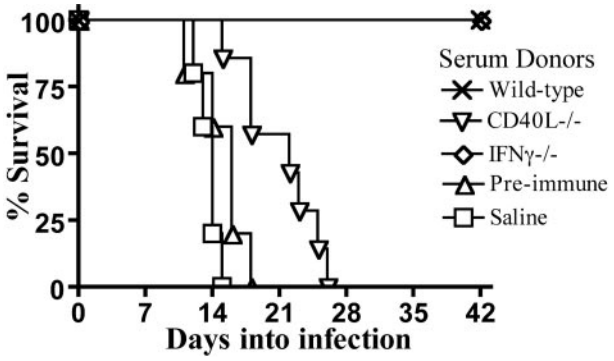

FIG. 5. Transfer of acute-phase serum to CD4$^{-/-}$ recipients. Shown are results from CD4$^{-/-}$ mice receiving saline (squares; 5 mice), preimmune serum from naïve C57BL/6 mice (triangles; 5 mice), or serum from acutely infected wild-type (crosses; 5 mice), CD40L$^{-/-}$ (inverted triangles; 7 mice), or IFN-$\gamma^{-/-}$ mice (diamonds; 5 mice). The crosses (representing wild type) and diamonds (representing IFN-$\gamma^{-/-}$ donors) overlap.

Adoptive transfer of CD4$^+$ T cells protects CD4$^{-/-}$ recipients against infection with *C. rodentium*. To determine the specific contributions of CD4$^+$ T-cell-expressed CD28, CD40L, and IFN-γ, we adoptively transferred 5 million wild-type or specifically deficient CD4$^+$ T cells into CD4$^{-/-}$ recipients subsequently infected with *C. rodentium*. Transfer of CD45.1$^+$ CD4$^+$ T cells to CD45.2$^+$ CD4$^{-/-}$ donors assessed the degree of reconstitution in uninfected and infected recipient mice 2 weeks after transfer (Table 1). Subsequent transfers used CD45.2$^+$ CD4$^+$ T cells from wild-type, CD28$^{-/-}$, CD40L$^{-/-}$, or IFN-$\gamma^{-/-}$ donors. Recipients receiving CD4$^+$ CD28$^-$ T cells demonstrated poor reconstitution of the CD4$^+$ T-cell compartment in spleen, MLN, and colon 2 weeks after transfer (Table 1), while recipients of CD4$^+$ CD40L$^-$ T cells demonstrated slightly improved reconstitution of the spleen and MLN but limited reconstitution of the colon (Table 1).

Adoptive transfer produced profound phenotypic effects upon survival of *C. rodentium* infection. Eighty percent of CD4$^{-/-}$ recipients receiving wild-type CD4$^+$ T cells successfully resolved infection (Fig. 6A). Transfer of CD4$^+$ CD28$^-$ T

TABLE 1. Percent $CD3^+$ $CD4^+$ T cells per total $CD3^+$ T cells in adoptively transferred $CD4^{-/-}$ recipients

Sample	% $CD3^+$ $CD4^+$ T cells/total $CD3^+$ T cells in recipient:[a]				
	C57BL/6 (no cells transferred; day 15 of infection)	$CD4^{-/-}$			
		$CD4^+$ T cells transferred		$CD4^+$ $CD28^-$ T cells transferred (day 15 of infection)	$CD4^+$ $CD40L^-$ T cells transferred (day 15 of infection)
		Uninfected	Day 15 of infection		
Spleen	54.9 ± 3.8	2.9 ± 0.5	13.5 ± 3.1	1.6 ± 0.5	8.0 ± 1.6
MLN	61.6 ± 8.6	2.4 ± 0.4	14.6 ± 2.8	1.3 ± 0.4	4.8 ± 0.5
Colon	55.1 ± 4.5	<1	28.8 ± 5.0	2.3 ± 1.3	3.5 ± 1.2

[a] The values represent [($CD3^+$ $CD4^+$ T cells)/(total $CD3^+$ T cells)] · 100 ± standard deviation.

cells produced survival comparable to that with control $CD4^{-/-}$ mice receiving media (14.8 days; Fig. 6B and E), while transfer of $CD4^+$ $CD40L^-$ T cells extended the mean survival to 20.7 days (Fig. 6C). Surprisingly, transfer of $CD4^+$ IFN-γ^- T cells (Fig. 6D) produced survival comparable to that of mice receiving wild-type $CD4^+$ T cells.

The differences in survival were associated with development of a protective profile of acute-phase serum antibody. Recipients transferred with wild-type $CD4^+$ T cells demonstrated acute pathogen-specific serum IgM comparable to that with wild-type mice and near-normal levels of IgG2b and IgG2c (Fig. 7, inverted triangles). Mice receiving $CD4^+$ $CD28^-$ T cells demonstrated poor pathogen-specific responses (Fig. 7, diamonds). Though transfer of $CD4^+$ $CD40L^-$ T cells produced a mild elevation in pathogen-specific IgM (Fig. 7, circles) and IgG2b (Fig. 7, circles), pathogen-specific IgM remained >5-fold lower and pathogen-specific IgG 10-fold lower than the titers found in mice receiving wild-type $CD4^+$ T cells (Fig. 7). Transfer of $CD4^+$ IFN-γ^- T cells resulted in comparable titers of total pathogen-specific serum IgM and IgG with compensatory titers of IgG2b (Fig. 7B, asterisks) and IgG3 (Fig. 7D, asterisks) in the absence of detectable IgG2c (Fig. 7C).

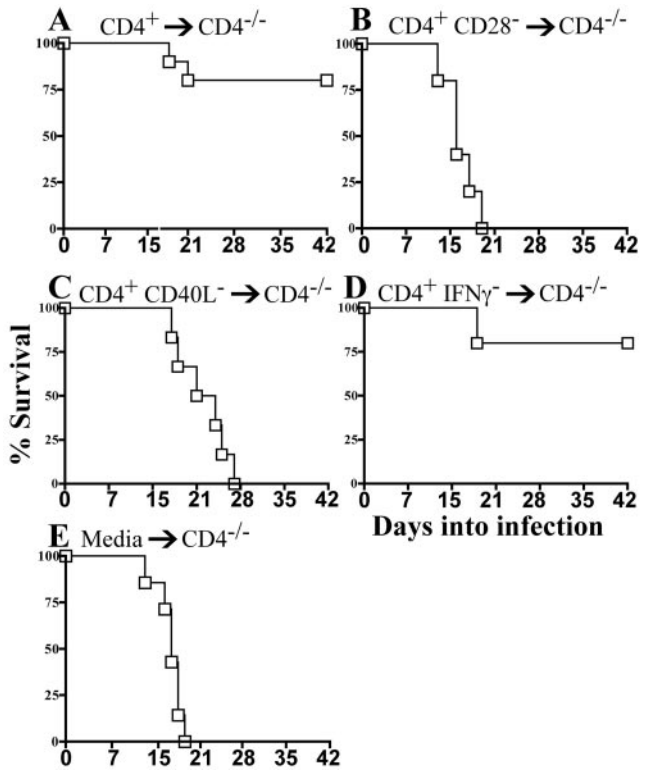

FIG. 6. Survival of $CD4^{-/-}$ mice adoptively transferred with $CD4^+$ T cells from wild-type or CD28-, CD40L-, or IFN-γ-deficient donors. (A) Mice receiving wild-type $CD4^+$ T cells ($n = 10$ mice). (B) $CD4^+$ $CD28^-$ T cells ($n = 5$ mice). (C) $CD4^+$ $CD40L^-$ T cells ($n = 6$ mice). (D) $CD4^+$ IFN-γ^- T cells ($n = 5$ mice). (E) $CD4^{-/-}$ recipients receiving media ($n = 8$ mice).

These titers correlated with lower pathogen burdens at day 15 of infection in internal organs. Transfer of wild-type $CD4^+$ T cells or $CD4^+$ IFN-γ^- T cells produced a ≥2-log decrease in the number of pathogenic bacteria found in the spleen when compared with $CD4^{-/-}$ mice receiving $CD4^+$ $CD28^-$ T cells or media (Fig. 8A; $P < 0.01$). Though recipients receiving $CD4^+$ $CD40L^-$ T cells developed lower mean burdens in spleen than $CD4^{-/-}$ mice, this difference was not significant ($\log_{10}$ CFU of *C. rodentium*/gram of tissue of 3.6 versus 4.3; $P = 0.06$).

DISCUSSION

Our findings have further elucidated the complicated interplay between mucosal and systemic adaptive immunity in controlling a primary infection of a mucosal surface. Unlike phylogenetically related members of the *Enterobacteriaceae* including *Salmonella enterica* serovar Typhimurium, *Shigella*, and enteric *Yersinia* species, *C. rodentium* does not establish a primarily invasive or intracellular infection. However, the infections caused by each of these pathogens involve contact with epithelial surfaces and the potential for direct microbial or host-mediated damage to the mucosa (3, 23). The adherence of high bacterial burdens of enteropathogenic *E. coli* or of *C. rodentium* to mucosal surfaces makes this process all the more important in the pathogenesis of infections caused by attaching and effacing pathogens. Epithelial disruptions provide passive portals through which pathogenic and commensal species may enter, creating the potential for polymicrobial sepsis. This microbiological "bystander effect" remains an underappreciated pathological mechanism that can occur with any process damaging the gut epithelial barrier and can contribute to the morbidity and mortality of mucosal infections in immature and immunocompromised populations (2, 6).

Adaptive immunity to *C. rodentium* requires development of a systemic and $CD4^+$ T-cell-dependent antibody response. This response is necessary in mice infected at the weaning

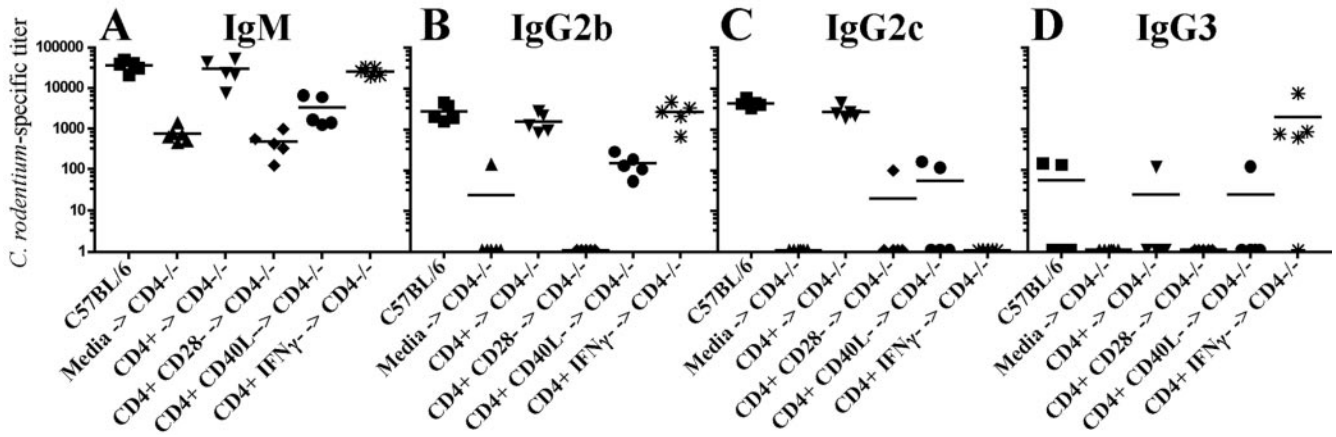

FIG. 7. Acute antibody responses in adoptively transferred $CD4^{-/-}$ mice. Shown are pathogen-specific IgM (A), IgG2b (B), IgG2c (C), and IgG3 (D) antibody responses. The *x* axis indicates antibody responses in wild-type, $CD4^{-/-}$, or adoptively transferred $CD4^{-/-}$ recipients; The *y* axis indicates the relative endpoint titer. The minimum detectable titer is 50. Squares, wild-type C57BL/6 mice; triangles, $CD4^{-/-}$ recipients receiving medium only; inverted triangles, $CD4^{-/-}$ recipients receiving wild-type CD4 T cells; diamonds, $CD4^{-/-}$ recipients receiving $CD28^{-/-}$ $CD4^+$ T cells; circles, $CD4^{-/-}$ recipients receiving $CD40L^{-/-}$ $CD4^+$ T cells; asterisks, $CD4^{-/-}$ recipients receiving IFN-$\gamma^{-/-}$ $CD4^+$ T cells.

transition or at older ages (2, 25). As demonstrated in mice lacking β_7-integrins, these responses need not occur in proximity to the primary mucosal site of infection

During primary infection with *C. rodentium*, CD28 clearly affects the in vivo survival and proliferation of $CD4^+$ T-helper cells, impacting downstream effector functions and development of protective antibody. More significantly, $CD4^+$ T-cell-expressed CD40L provides a key costimulatory effector function needed to develop protective antibody responses. While more than half of $CD40L^{-/-}$ mice, or $CD4^{-/-}$ mice receiving serum from $CD40L^{-/-}$ donors, survived the normal period of acute infection, animals failed to resolve colonic infection and ultimately succumbed to profound polymicrobial sepsis. As systemic IgG responses have been implicated in the clearance of colonic *C. rodentium* (15), the lack of reactive IgG in $CD40L^{-/-}$ mice could explain this protracted course of infection among $CD40L^{-/-}$ mice and $CD4^{-/-}$ mice receiving serum or $CD4^+$ $CD40L^-$ T cells from $CD40L^{-/-}$ donors.

Surprisingly, deficiency of IL-4 or of $CD4^+$ T-cell-produced IFN-γ did not adversely impact the host's ability to develop protective antibody and survive infection. The roles played by IL-4 or $CD4^+$ T-cell-expressed IFN-γ in the resolution of this infection may thus be small, or alternatively they may be overcome through other mechanisms in the deficient host. Furthermore, IFN-γ produced by populations other than $CD4^+$ T cells, including NK cells, neutrophils, macrophages, or dendritic cells, may promote key effector functions needed for host defense, including macrophage activation, neutrophil recruitment, and aspects of epithelial defense, including the induction of antimicrobial defensins (19, 24).

However, the profile of protective antibody generated in wild-type mice indicates the development of IFN-γ and other cytokine responses in a normal host. The dependence of the IgG2c response on $CD4^+$ T-cell-expressed IFN-γ demonstrates that immunocompetent mice generate Th1 responses during mucosal infection with *C. rodentium*. The codevelopment of *Citrobacter*-specific IgG2b, an IgG isotype promoted by transforming growth factor β1 (5, 17), further suggests contributions of regulatory cytokine responses. Dissecting the manner and locations in which these responses develop may be key to discerning how the normal host evolves and controls proinflammatory responses generated during mucosal infections.

Protective serum antibody responses in acute infection consisted of pathogen-specific IgM with evolving IgG2b/IgG2c or IgG2b/IgG3 responses. These profiles are consistent with complement-fixing antibodies and convalescent IgG responses that bind with high affinity to myeloid FcγR1 receptors and FcγRII/III receptors (20). Whereas pathogen-specific IgM develops during the point in infection when a naïve host is most susceptible to the development of sepsis, pathogen-specific IgG, and not mucosal IgA, has been demonstrated to help clear the

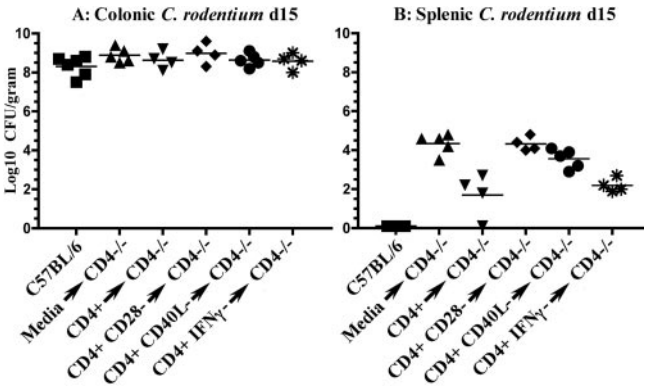

FIG. 8. Burden of *C. rodentium* in adoptively transferred $CD4^{-/-}$ mice. Shown are colonic (A) and splenic (B) CFU of *C. rodentium* at 15 days of infection. The *y* axis denotes $\log_{10}$ CFU of *C. rodentium* per gram of tissue. The *x* axis indicates the mouse strain and cell populations transferred to $CD4^{-/-}$ mice. Squares, wild-type C57BL/6 mice; triangles, $CD4^{-/-}$ recipients receiving medium only; inverted triangles, $CD4^{-/-}$ recipients receiving wild-type CD4 T cells; diamonds, $CD4^{-/-}$ recipients receiving $CD28^{-/-}$ $CD4^+$ T cells; circles, $CD4^{-/-}$ recipients receiving $CD40L^{-/-}$ $CD4^+$ T cells; asterisks, $CD4^{-/-}$ recipients receiving IFN-$\gamma^{-/-}$ $CD4^+$ T cells.

colonic infection (15). Our data demonstrate that reactive IgG, IgG2b in particular, enters the lumen through an ill-defined mechanism, whether through damaged or leaky epithelium, FcRn-mediated epithelial transport, or uptake and release via the hepatobiliary system (22, 27). Effector functions of reactive antibody could thus include a combination of complement-mediated, phagocytic and direct antimicrobial functions, acting in systemic and mucosal locations.

We have defined key effector functions of $CD4^+$ T cells during infection with the attaching and effacing pathogen *C. rodentium*. $CD4^+$ T-cell-expressed CD28 and CD40L promote the development of protective humoral immunity during this primary infection of a mucosal surface, while deficiency of IL-4 or $CD4^+$ T-cell-expressed IFN-γ have limited functional effects. These systemic adaptive immunological responses are essential for control of infections previously thought to be localized to the gastrointestinal tract. The development of a $CD4^+$ T-cell adoptive transfer model with a robust survival phenotype provides a powerful tool to further dissect the evolution of differential Th responses in mucosal and systemic locations and to study $CD4^+$ T-cell and antibody-mediated processes leading to successful resolution of mucosal infections and associated inflammation.

ACKNOWLEDGMENTS

We thank Shannon Bowes and Monica Wang for technical assistance and Terry and David Bowman for histological processing.

This work was supported by funding from NIH grants R01 AI38578, K08 AI051734, and R21 AI059628. L.B. is a recipient of a K08 Career Development Award from the National Institutes of Health.

REFERENCES

1. **Bertram, E. M., A. Tafuri, A. Shahinian, V. S. Chan, L. Hunziker, M. Recher, P. S. Ohashi, T. W. Mak, and T. H. Watts.** 2002. Role of ICOS versus CD28 in antiviral immunity. Eur. J. Immunol. **32:**3376–3385.
2. **Bry, L., and M. B. Brenner.** 2004. Critical role of T cell-dependent serum antibody, but not the gut-associated lymphoid tissue, for surviving acute mucosal infection with *Citrobacter rodentium*, an attaching and effacing pathogen. J. Immunol. **172:**433–441.
3. **Clark, M. A., B. H. Hirst, and M. A. Jepson.** 1998. M-cell surface β1 integrin expression and invasin-mediated targeting of *Yersinia pseudotuberculosis* to mouse Peyer's patch M cells. Infect. Immun. **66:**1237–1243.
4. **Cleary, J., L. C. Lai, R. K. Shaw, A. Straatman-Iwanowska, M. S. Donnenberg, G. Frankel, and S. Knutton.** 2004. Enteropathogenic *Escherichia coli* (EPEC) adhesion to intestinal epithelial cells: role of bundle-forming pili (BFP), EspA filaments and intimin. Microbiology **150:**527–538.
5. **Deenick, E. K., J. Hasbold, and P. D. Hodgkin.** 1999. Switching to IgG3, IgG2b, and IgA is division linked and independent, revealing a stochastic framework for describing differentiation. J. Immunol. **163:**4707–4714.
6. **DeMeo, M. T., E. A. Mutlu, A. Keshavarzian, and M. C. Tobin.** 2002. Intestinal permeation and gastrointestinal disease. J. Clin. Gastroenterol. **34:**385–396.
7. **Deng, W., Y. Li, B. A. Vallance, and B. B. Finlay.** 2001. Locus of enterocyte effacement from *Citrobacter rodentium*: sequence analysis and evidence for horizontal transfer among attaching and effacing pathogens. Infect. Immun. **69:**6323–6335.
8. **Deng, W., B. A. Vallance, Y. Li, J. L. Puente, and B. B. Finlay.** 2003. *Citrobacter rodentium* translocated intimin receptor (Tir) is an essential virulence factor needed for actin condensation, intestinal colonization and colonic hyperplasia in mice. Mol. Microbiol. **48:**95–115.
9. **Goncalves, N. S., M. Ghaem-Maghami, G. Monteleone, G. Frankel, G. Dougan, D. J. M. Lewis, C. P. Simmons, and T. T. MacDonald.** 2001. Critical role for tumor necrosis factor alpha in controlling the number of lumenal pathogenic bacteria and immunopathology in infectious colitis. Infect. Immun. **69:**6651–6659.
10. **Higgins, L. M., G. Frankel, G. Douce, G. Dougan, and T. T. MacDonald.** 1999. *Citrobacter rodentium* infection in mice elicits a mucosal Th1 cytokine response and lesions similar to those in murine inflammatory bowel disease. Infect. Immun. **67:**3031–3039.
11. **Johnson-Leger, C., J. R. Christenson, M. Holman, and G. G. Klaus.** 1998. Evidence for a critical role for IL-2 in CD40-mediated activation of naive B cells by primary CD4 T cells. J. Immunol. **161:**4618–4626.
12. **Lens, S. M., P. A. Baars, B. Hooibrink, M. H. van Oers, and R. A. van Lier.** 1997. Antigen-presenting cell-derived signals determine expression levels of CD70 on primed T cells. Immunology **90:**38–45.
13. **Li, C. K., S. L. Pender, K. M. Pickard, V. Chance, J. A. Holloway, A. Huett, N. S. Goncalves, J. S. Mudgett, G. Dougan, G. Frankel, and T. T. MacDonald.** 2004. Impaired immunity to intestinal bacterial infection in stromelysin-1 (matrix metalloproteinase-3)-deficient mice. J. Immunol. **173:**5171–5179.
14. **Luperchio, S. A., and D. B. Schauer.** 2001. Molecular pathogenesis of *Citrobacter rodentium* and transmissible murine colonic hyperplasia. Microbes Infect. **3:**333–340.
15. **Maaser, C., M. P. Housley, M. Iimura, J. R. Smith, B. A. Vallance, B. B. Finlay, J. R. Schreiber, N. M. Varki, M. F. Kagnoff, and L. Eckmann.** 2004. Clearance of *Citrobacter rodentium* requires B cells but not secretory immunoglobulin A (IgA) or IgM antibodies. Infect. Immun. **72:**3315–3324.
16. **MacDonald, T. T., G. Frankel, G. Dougan, N. S. Goncalves, and C. Simmons.** 2003. Host defences to Citrobacter rodentium. Int. J. Med. Microbiol. **293:**87–93.
17. **McIntyre, T. M., D. R. Klinman, P. Rothman, M. Lugo, J. R. Dasch, J. J. Mond, and C. M. Snapper.** 1993. Transforming growth factor beta 1 selectivity stimulates immunoglobulin G2b secretion by lipopolysaccharide-activated murine B cells. J. Exp. Med. **177:**1031–1037.
18. **Mundy, R., D. Pickard, R. K. Wilson, C. P. Simmons, G. Dougan, and G. Frankel.** 2003. Identification of a novel type IV pilus gene cluster required for gastrointestinal colonization of *Citrobacter rodentium*. Mol. Microbiol. **48:**795–809.
19. **Ohteki, T., T. Fukao, K. Suzue, C. Maki, M. Ito, M. Nakamura, and S. Koyasu.** 1999. Interleukin 12-dependent interferon gamma production by CD8alpha+ lymphoid dendritic cells. J. Exp. Med. **189:**1981–1986.
20. **Ravetch, J. V., and J. P. Kinet.** 1991. Fc receptors. Annu. Rev. Immunol. **9:**457–492.
21. **Rogers, P. R., and M. Croft.** 2000. CD28, Ox-40, LFA-1, and CD4 modulation of Th1/Th2 differentiation is directly dependent on the dose of antigen. J. Immunol. **164:**2955–2963.
22. **Roopenian, D. C., G. J. Christianson, T. J. Sproule, A. C. Brown, S. Akilesh, N. Jung, S. Petkova, L. Avanessian, E. Y. Choi, D. J. Shaffer, P. A. Eden, and C. L. Anderson.** 2003. The MHC class I-like IgG receptor controls perinatal IgG transport, IgG homeostasis, and fate of IgG-Fc-coupled drugs. J. Immunol. **170:**3528–3533.
23. **Sansonetti, P. J., J. Arondel, M. Huerre, A. Harada, and K. Matsushima.** 1999. Interleukin-8 controls bacterial transepithelial translocation at the cost of epithelial destruction in experimental shigellosis. Infect. Immun. **67:**1471–1480.
24. **Simmons, C. P., N. S. Goncalves, M. Ghaem-Maghami, M. Bajaj-Elliott, S. Clare, B. Neves, G. Frankel, G. Dougan, and T. T. MacDonald.** 2002. Impaired resistance and enhanced pathology during infection with a noninvasive, attaching-effacing enteric bacterial pathogen, Citrobacter rodentium, in mice lacking IL-12 or IFN-gamma. J. Immunol. **168:**1804–1812.
25. **Simmons, C. P., S. Clare, M. Ghaem-Maghami, T. K. Uren, J. Rankin, A. Huett, R. Goldin, D. J. Lewis, T. T. MacDonald, R. A. Strugnell, G. Frankel, and G. Dougan.** 2003. Central role for B lymphocytes and $CD4^+$ T cells in immunity to infection by the attaching and effacing pathogen *Citrobacter rodentium*. Infect. Immun. **71:**5077–5086.
26. **Spahn, T. W., C. Maaser, L. Eckmann, J. Heidemann, A. Lugering, R. Newberry, W. Domschke, H. Herbst, and T. Kucharzik.** 2004. The lymphotoxin-beta receptor is critical for control of murine *Citrobacter rodentium*-induced colitis. Gastroenterology **127:**1463–1473.
27. **Spiekermann, G. M., P. W. Finn, E. S. Ward, J. Dumont, B. L. Dickinson, R. S. Blumberg, and W. I. Lencer.** 2002. Receptor-mediated immunoglobulin G transport across mucosal barriers in adult life: functional expression of FcRn in the mammalian lung. J. Exp. Med. **196:**303–310.
28. **Uren, T. K., O. L. Wijburg, C. Simmons, F. E. Johansen, P. Brandtzaeg, and R. A. Strugnell.** 2004. Vaccine-induced protection against gastrointestinal bacterial infections in the absence of secretory antibodies. Eur. J. Immunol. **35:**180–188.
29. **Walker, L. S., A. Gulbranson-Judge, S. Flynn, T. Brocker, C. Raykundalia, M. Goodall, R. Forster, M. Lipp, and P. Lane.** 1999. Compromised OX40 function in CD28-deficient mice is linked with failure to develop CXC chemokine receptor 5-positive CD4 cells and germinal centers. J. Exp. Med. **190:**1115–1122.
30. **Walker, L. S., A. Gulbranson-Judge, S. Flynn, T. Brocker, and P. J. Lane.** 2000. Co-stimulation and selection for T-cell help for germinal centres: the role of CD28 and OX40. Immunol. Today **21:**333–337.

Editor: A. D. O'Brien